

Application of High-Resolution 3D Scanning in Medical Volumetry

Adam Chromy

Abstract—This paper deals with application of 3D scanning technology in medicine. Important properties of 3D scanners are discussed with emphasize on medical applications. Construction of medical 3D scanner according to these specifications is described and practical application of its use in medical volumetry is presented. Besides volumetry, such 3D scanner is usable for many other purposes, like monitoring of recovery process, ergonomic splint manufacturing or inflammation detection.

3D scanning introduces novel volumetric method, which is compared with standard methods. The new method is more accurate compared to present ones. Principles of this method are discussed in paper and its accuracy is evaluated and experimentally verified.

Keywords—medical volumetry, medical 3D scanning, 3D scanning, medical imaging, soft-tissues

I. INTRODUCTION

Capturing three-dimensional models has become more and more important during last years, due to rapid development of 3D technologies, especially 3D printers. They are very frequently requested devices today, its market is rapidly growing and its development also moves forward very fast. According to Google Trends, number of search queries related to 3D technologie increased more than ten times during last three years [1]. Architectural models of buildings, design prototypes of new products, or even 3D printers itself are 3D printed today. There are experiments with printing real houses, food, or bioprinting [2]. All these applications require the same – **computer 3D model**.

3D printing is not the only domain, where 3D models are useful. They can be also used for *storing visual information* in compact and resistant form, in which the objects are not ageing. In this case, colour-covered 3D models seem to be the best modality. E.g. The Metropolitan Museum of Art published models of its exhibits [3], or South Korea archived its UNESCO heritage areas [4].

Finally, computer 3D models are, due to its plasticity, becoming more and more used for *visualization of objects*, which are unreachable (contaminated, dangerous or remote areas) [5], [6] or environments, which are invisible without invasive surgery (human inner structures) [7]. Another objects are visible, but its important details are too tiny (human outer structures) and it is necessary to enlarge them plastically [8].

This work was supported by the grant No. FEKT-S-14-2429 The research of new control methods, measurement procedures and intelligent instruments in automation financed from internal science fund of Brno University of Technology.

Author is with Faculty of Electrical Engineering and Communication, Brno University of Technology, Brno, Czech Republic (e-mail: adam.chromy@ceitec.vutbr.cz).

There are several possibilities of capturing such 3D models, but the most frequent method is **3D scanning**, what means direct capturing of 3D model with device intended for this purpose [9]. This technology is spreading into the new domains and more and more new applications are announced each year. But still, there are mostly technical domains getting involved. The medicine is one of domains, where 3D models are very rarely used, even though many opportunities of potential 3D scanning applications exist.

This paper deals with applications of 3D scanning technologies in medicine, with focus on one of the areas, where 3D scanning brings significant advantages – on **Medical Volumetry**.

Observing parameters of human body volumes has been one of the most important factors in diagnosis since beginnings of medicine and has also served for evaluation of suitability of applied therapy. But if you are visually observing only, all these geometrical changes can be useful once the symptoms are large, what typically means that the disease is already developed.

To be able to reveal the disease in its *very beginning*, it is not enough to observe only, it needs to *measure* and even with as high as possible resolution, what provides possibility of early detection of tiny changes of volumes, which refer to symptoms of disease.

In this study, we are focused on application of precise 3D scanning for accurate measurements of volumetric parameters, primarily body-part volume. To know the exact value of this parameter is valuable for many purposes – e.g. early detection of peripheral oedemas [10], lymphedemas, carcinomas [11] or fibrosis [12], its monitoring and control of its evolution; measurement of influence of strength exercises on sportsmen [13] or supervision of recovery process after invasive surgeries [14]. Present standard methods are not accurate enough, easily usable, or require high operational expenses.

Precise 3D scanning has also one extra advantage – spatial resolution of such models can be also enlarged by one dimension and all these models could be registered in relation to time. With 3D scanning, we are not able to precisely measure only, we are also able to see trends.

In this paper, the present volumetric methods are summarized, then constitution of the best suitable 3D scanner for medical purposes is discussed and its practical application in medical volumetry is presented. Finally, this new volumetric method is compared with present ones, both theoretically and experimentally.

II. PRESENT VOLUMETRIC METHODS

According to [11], [13], [15]–[17], the most frequently used volumetric methods are:

A. Circumferential measurements

Methods of this group are based on volume estimation from measurements of circumference at several specific places. Every method uses some form of surface approximation, what leads to lower accuracy [16]. Repeatability of measurements significantly depends on experience of person performing measurement [18]. On the other hand, no special equipment is required, they are simple and useful for non-flexible limbs and patients with bad motoric abilities or water incompatible diseases [11].

The first most used method is *Frustum Sign Model* based on measurements of 2 circumferences and approximation by truncated cone between them, with relative accuracy¹ about $\pm 8\%$ of measured volume [18]. Even though its accuracy is low, its extremely fast (less than 1 min.), what makes it suitable for situations, where quick estimation of volume, without emphasis on accuracy, is required [19].

Second method called *Disc Model* estimates volume as sum of equidistant disks with distance of 5 cm, with relative accuracy about $\pm 6\%$ of measured volume [18], but be aware, that all these accuracies must not be considered as definitive since significantly depends on personal experiences.

B. Water Displacement Volumetry

The most used volumetric method, considered as golden standard [13], is based on quantum of water overflowing from fully filled container when measured limb is inserted. It is frequently used because of its good accuracy, very good repeatability and negligible dependency on operator's experiences comparing to circumferential measurements. The biggest disadvantages are, that it requires good flexibility and good motoric abilities of measured limb (shivering of limb significantly influences result), there is possible risk of cross-infection, some patients have to avoid water because of their disease and it is very time consuming [11], [15]. According to [13], [18], [20], its relative accuracy is inversely proportional with measured object volume and varies from $\pm 2\%$ in case of lower leg measurements (about 2700 cm³) to $\pm 8\%$ in case of finger measurements (about 25 cm³).

C. Optoelectronic Volume Measurement

There are several commercially available single-purpose volumetric devices using this method. The measurement principle is based on horizontally movable frame equipped with infrared light emitters and receptors. This frame is moving along axis of examined limb. Light beams are interrupted by the volume of measured limb and the shadow is captured at receptors in two perpendicular axes. By moving the frame, many measurements are performed and volume is then calculated from these values [18]. According to [20] relative

¹term "relative accuracy" in this paper means relative uncertainty with 95% confidence (2σ)

accuracy of such device is $\pm 2\%$ of measured volume (in case of measurements in range from 1000 to 3000 cm³), but the repeatability is much better since the measured value is not too dependant on personal experiences or motoric abilities of patient [16]. Disadvantage of this method is, that expensive, single-purpose device is required and resultant benefits are not too significant compare to Water Displacement Volumetry, which is much cheaper [10].

D. 3D Sonography, CT and MRI

In very occasional cases, mostly for research purposes, the volume is computed from 3D models provided by these three-dimensional imaging modalities [21]–[24]. Each of them is able to provide 3D model of body part, but each of them has significant disadvantages disallowing its usage in common health care. *Ultrasonography*, due to its divergence of sound-beam, has too poor resolution (about 5 mm) to be better than simple Circumferential or Water displacement methods [25]. Among this, it has too noisy image [26]. *Computed Tomography (CT)* reaches up to 0.2 mm spatial resolution in output 3D model [27], but ionizing radiation absorbed by patient during one scan is up to 15 mSv, what is one third of allowed exposition for workers with ionizing source per year and for common people exceeds allowed hygiene limits even 15 times [28]. For this reason, use of this modality is allowed as rare as possible and repeated scanning is completely out of the question. Finally, *Magnetic Resonance Imaging (MRI)*, although its resolution is approx. 1 mm, cannot be widely used because of its high costs, time consuming examinations, pacemaker or piercing disallowing [29].

Application of 3D scanning in medicine brings novel volumetric method, which reaches of better accuracy than mentioned volumetric methods, good repeatability, easy use and low operational costs.

III. 3D SCANNERS

There are plenty of 3D scanners working on various principles, so their review would take a whole book. But what they have common is, that we can make a list of modules, which each scanner must have somehow implemented. Rather than evaluating each model of 3D scanner, we discuss each available implementation of every module with emphasize on medical application of 3D scanner. By choosing the most suitable implementation of each functional block, we can make an image, how the ideal medical 3D scanner should be realized.

There are blocks, which each scanner consists of:

A. Raw Data Capturing

The most of scanners measure distance of surface from sensor. In case of *contact scanners*, this distance is given by length of touch probe. This can be very precise, but touching the examined object can be damaging or frustrating (in case of human body scanning) [30].

Contactless techniques are mostly using the laser beam (*laser scanners*). Solution with measuring the *time of flight* of

laser quantum provides wide measuring range (up to hundreds of meters), but its precision is limited by resolution of time-measuring unit (up to 1 mm) [31]. Another laser scanner principle is *triangulation*, having opposite abilities: its accuracy is very high (up to 1 μm [32]), but its measuring range is limited (hundreds of millimetres [33]). The *interferometric laser scanner* reaches up to 1 μm resolution, but its range is up to hundreds of μm [34].

Structured-light 3D scanners project a pattern of light on the subject and look at its deformation in captured image [35]. The advantage of this method is high speed of scanning since each time the entire image is analysed instead of one point [36]. Another advantage is the precision, which is even better than laser triangulation [37].

Stereophotogrammetric scanners use two cameras to estimate 3D position of points from differences between two images. It is also quite fast with accuracy up to 1 mm [38].

Different type of raw data capture MRI and CT, where the value relevant to density of material, is measured in every place of examined region. MRI measurements are very slow (tens of minutes), but inner structures of human body are visualized (with spatial resolution approx. 1.5 mm^3) [21], [22]. Slightly faster and more accurate (approx. 0.6 mm^3) is CT [27], but its important disadvantage is ionizing radiation.

B. Moving the Sensor

In order to build a 3D model of arbitrarily complex object, the sensor must be positioned to several view-points, from which all details on the surface of object are visible [39].

The *hand-held scanners* are devices, where moving of sensor along scanning trajectory is realised manually [40]. It reaches the best flexibility, but the task of sensor localization (see next section) is complicated [41].

The majority of 3D scanners use *motorized sensor moving*, mostly composed from precise electric stepper drive [42] or servomotor [43]. It provides automatic movements along optimal, pre-tested trajectories and empowers also easier sensor localization. It also minimizes the problem with scanning ranges, which can be very narrow in some cases (e.g. triangulation laser scanners) and to stay manually in this range can be difficult. Disadvantage is, that flexibility of movement is limited by the kinematic conception of axes, along which the sensor moves [44]. The best flexibility reaches the articulated kinematic chain with at least 6 DOF. When adding 7th degree of freedom, the singularity problems are minimized [45].

C. Sensor Localization

To be able to resolve position of measured point in coordinate system, it is necessary to know the precise position of sensor in 6 DOF² (among raw data itself).

This task is simple in cases, when motorized sensor positioning is used, since the sensor must be connected to moveable axis by joints³, which position can be simply measured

²3 coordinates unambiguously define position of point and another 3 coordinates unambiguously define its orientation

³Joint in this sense can be also linearly translational, not only rotational

by encoders, resolvers [46], servomotoric feed-back [43], etc. Using *direct kinematics*, its position can be unambiguously computed with high precision [47].

Free hand-held scanners use the *image registration* to estimate its location alteration from change of scene between last two scans [48]. Many scanners use some method based on ICP [49], usually optimized [50] or modified for specific application [51]–[53]. This approach has two disadvantages: The absolute accuracy is very low, due to cumulative character of localizing algorithm, which sums partial errors [54]. It can also fail in uniform scenes like a plane, cylinder, sphere, etc. This problem can be partly minimized by external localizing system based on inertial measurement unit (IMU) [41], or fully solved by use of passive kinematic chain with joint measurements [55].

D. Planning Trajectory of Sensor

There are 3 types of scanning trajectory planning: online, static and adaptive.

Online planning is typical for hand-held scanners, since the exact trajectory is created just when scanning and is unknown before [40]. The result depends on operator skills (if he meets the measuring range, if scanning just the region of interest, etc.). The other special example of online planning is autonomous planning of trajectory based on extra system measurements (e.g. overview laser scanner) [56]. Even though many publication have been published on this topic, the solution are still not enough robust to be commonly used [57].

Static planning uses predefined and pre-tested scanning trajectories. They are simple and robust in sense of no risk of unexpected behaviour of positioning system [58]. On the other hand, their use is non-flexible and limited e.g. with sensors with narrow measuring range. Trajectories must be frequently redefined also in case of slight differences of scanned objects.

Adaptive planning combines both methods above. The general concept of trajectory is strictly defined, but slight, on-line computed deviations according to scanned object are allowed (Fig. 1) [58]. Since the changes of trajectory are allowed just in defined degree of freedom and also limited, there is no risk of unexpected moving and the algorithm is more flexible.

E. Computation of 3D Point Position

The contact scanners dispose with the easiest way of 3D point computation, since the position of touched point is directly the sensor location, only shifted by the length of probe [30].

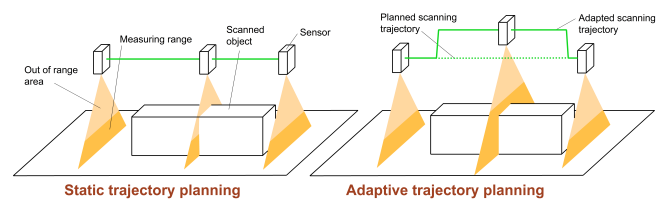


Fig. 1. Illustrating difference between Static planning and Adaptive planning.

The most of 3D scanner types use *geometric transformations* to build the 3D model. This technique can be used, when captured raw data contains any spatial information (e.g. distance measured by laser scanner) or are spatially ordered (voxels of CT and MRI).

In case of *stereophotogrammetry*, the transformation approach cannot be used, since there is no spatial information in the raw captured data. The three-dimensional representation of scanned object must be inferred from two images captured with two cameras watching the same scene from different views [48].

F. Storing and Visualization of 3D Models

There are two basic approaches of storing three-dimensional data:

3D Grid divides spatial area of scanned object to regularly ordered same-size elements called voxels. Each cube contains probability of occupancy by object (Occupancy Grid [59]) or other value describing the voxel locality (Evidence Grid [60]), e.g. density in case of MRI or CT. All objects in scan are then approximated by number of same cubes, what is far from reality. Also the memory requirements are very high. On the other hand, computations over such model are simple and fast. Its useful for models in low resolution, which are frequently updated and rebuild, e.g. in case of 3D live view. This representation is used in standard medical file format DICOM, used for storing data from CT and MRI.

Point Cloud in its raw format is unordered set of three-dimensional vectors defining position of points in space [60]. In practical applications, they contains also extra informations about this point (colour, material, etc.). This format allows to describe the world by geometric shapes, what is more authentic approximation than grids. The memory requirements are significantly lower than grids. Disadvantage of this format is higher computational load and more complex analysing of model. Its useful for models, where precision and high resolution is required, but they are not updated too often [61].

IV. MEDICAL 3D SCANNER

The universal 3D scanning device suitable for medical purposes and usable in everyday practice shall have following abilities:

- *High accuracy* – essential parameter to being able to distinguish even tiny changes of human body caused by oedemas, muscle atrophy or muscle strengthening.
- *Flexibility* – since device should be universal, we shall be capable of scanning entire body as same as its tiny details. Because of that, the 3D scanner must be very flexible.
- *Low operational costs* – to allow its everyday use, its operation shall be inexpensive.
- *Simple manipulation* – device must be as much as possible automated, not disturbing the personnel with complex settings before each scanning.
- *High speed* – the scanning procedure must be very fast. In other cases, the personnel would not have time to use it and would prefer estimation instead of measurement.

- *No limitations* – device should be usable with any patient. There should be no limitations according to metal parts, health state, etc.
- *Harmless operation* – using the device shall not be harmful for both patient and personnel in any circumstances.

To fulfil all these requirements, the design of medical 3D scanner shall be as follows:

Data capturing sensor shall be structured light 3D scanner or triangulation laser scanner, due to precision reasons. As a result of this, computation of 3D point position shall be based on geometric transformations. Sensor motion shall be motorized from reason of precise sensor localization, automatic movement and keeping in measuring range. The kinematic chain shall be articulated, due to the flexibility requirement. Trajectory planning shall be adaptive, in order to reach some degree of autonomy with keeping the motion under the control. Captured data shall be stored in form of extended point cloud, since it does not affect model accuracy. The problem with computational requirements is not serious, since the model is once captured and afterwards modified occasionally.

Because such device is not commercially available, we created our own 3D scanner [62] meeting the specifications above: Robotic 3D Scanner.

A. Robotic 3D Scanner

Robotic 3D scanner is a 3D modelling system based on novel constitution, which uses combination of 6 DOF industrial robotic manipulator and triangulation-based laser scanner connected with controlling and data processing computer (Fig. 2). Laser scanner measures distance from patient surface, when robotic manipulator controls scanner position and orientation. From information about position, direction of view and distance to surface, each point position in 3D space can be computed. This solution combines *high flexibility* with *high precision and reliability*.

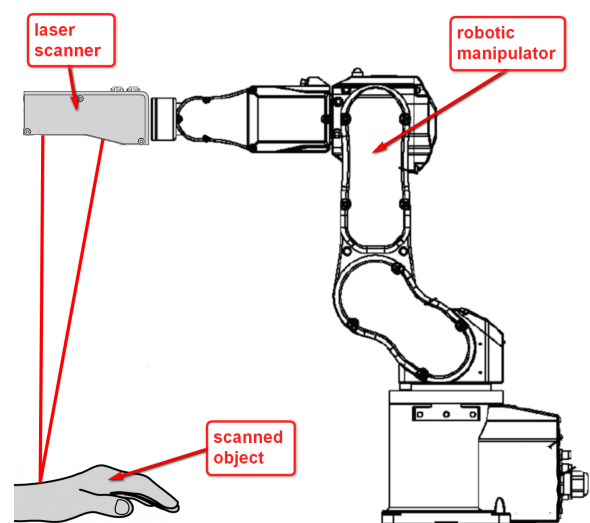


Fig. 2. Robotic manipulator with laser scanner combines high accuracy with flexibility.

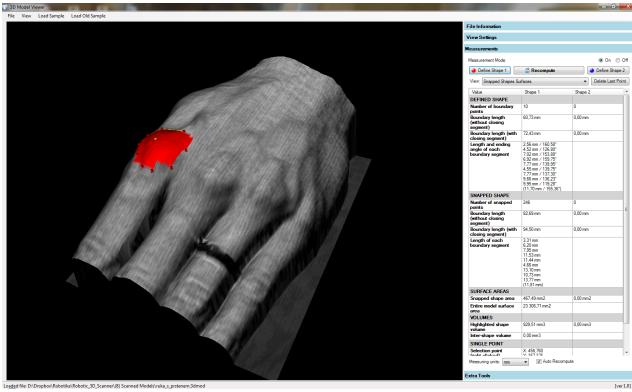


Fig. 3. Analyzing software allowing measurements of region of interest.

High accuracy is reached by using precise manipulator with accurate laser scanner and high flexibility is caused by programmable scanning trajectory in six degrees of freedom and by replaceability of laser scanner, what provides possibility of scanning both tiny and large structures.

It is 3D modelling system, useful for many different medical applications beside volumetrics: monitoring of tissue recovery process, pose measurements for rehabilitation purposes or ergonomic splints design; but also at other domains from archiving of historical materials in museums, through design, models for computer games and industrial inspection to 3D object cloning.

Robotic 3D Scanner provides three-dimensional model of patient body-part, which can be analyzed in ourself-developed analyzing software (Fig. 3). The big advantage is the possibility of selection of region of interest. There are several parameters available to be measured:

- Distances [mm] – between defined points (directly, along the surface), circumferences of ROI.
- Angles [deg] – angle between three defined points (e.g. vertebrae positions)
- Surface area [mm²] – entire model or ROI
- Volume [mm³] – entire model or ROI defined by cutting plane or deflected cutting surface

Detailed description of Robotic scanner's principles and functions, relevant transformation equations or analysing software capabilities can be found at [44] or [8].

V. NEW VOLUMETRIC METHOD

Contrary to Frustum Sign Model, Disc Model, Water Displacement Method and Optoelectronic Volumeters, what are the single-purpose methods or devices, this method applies multi-purpose Robotic 3D Scanner [44] in order to measure volume. Likewise the MRI or CT, it is not a device developed to measure volumes only, it is a universal 3D scanning device applicable for many other various purposes.

Robotic 3D Scanner Volumetry use the same measuring procedure as volumetry realized by MRI, CT or Ultrasonographic volumetry. The same measuring procedure is applied also in case of using any other generic 3D scanner, the only difference are properties of output values (accuracy, repeatability, region selectability, etc.).

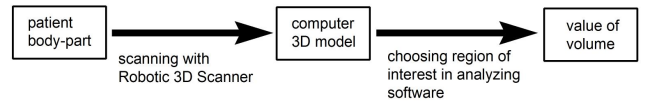


Fig. 4. Main principle of proposed volumetric method.

Method principle can be divided to several steps, as shown on Fig. 4.

First step is characterized by creating a precise 3D model of measured limb or any other interested body part. This model is stored in *point-cloud form*, which eliminates losses of detailed features and increases accuracy of the method ⁴.

Such models are visualized to operator, who defines regions of interest (ROI) whereof volume want to be measured (Fig. 3). This ability is an important advantage on contrary of some standard methods (e.g. Water Displacement Volumetry), where ROI is defined by method itself.

The volume of selected ROI is then computed. Robotic 3D Scanner Volumetry uses Signed Volume of Tetrahedron Method [63], which accuracy is limited only by positioning error of points of captured 3D model. Grid-based storing systems (MRI, CT, Sono) computes volume as sum of voxels⁵ belonging to ROI. Resulting accuracy is then limited by grid resolution.

A. Major Advantages of This Method

There are several major advantages of this method, compared to standard ones:

- *The highest accuracy* compare to standard methods (see section V-B).
- *Accuracy is independent* on skills of hospital staff, like it is not in case of Circumferential measurements.
- *Fast measuring process* compared to all the methods except the Optoelectronic volumeters.
- *No requirements on patient* like at Water Displacement Method (mobility and flexibility of limb) or MRI (no piercing, no pace-makers).
- *Multi-purpose imaging modality*, not single-purpose device as Optoelectronic volumeters.
- *Selectivity* of measured area (possible to define region of interest).
- *Low operation expenses* compare to CT or MRI.
- *No ionizing radiation* like at CT.

B. Accuracy of Measurement

As mentioned above, resulting volume is computed from three-dimensional model of object surface. When using point-cloud form and Signed Volume of Tetrahedron Method for volume computation, the only indispensable source of uncertainty is then uncertainty of measuring the position of single point

⁴MRI and CT principles do not allow to use a point-cloud form for storing informations, the grid-type memory must be used, what leads to decrease of method accuracy.

⁵Voxel is the smallest available volume element in grid representation. In most realizations, it is a cube with length of side given by spatial resolution.

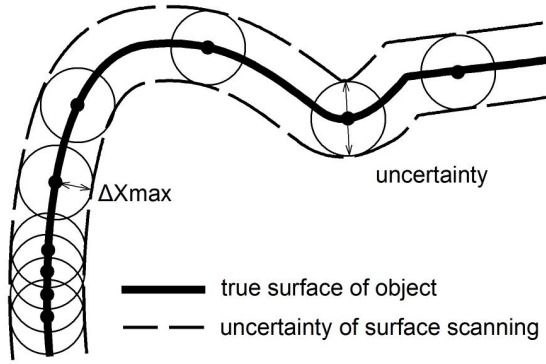


Fig. 5. Volumetric uncertainty: Deriving theoretical accuracy from laser scanning uncertainty.

in 3D model (Δ_{Xmax}). As long as the Robotic 3D Scanner is properly calibrated, the only considerable sources influencing scanner's accuracy are robotic manipulator accuracy (Δ_M) and laser scanner accuracy (Δ_S). Relation between these symbols has been derived in [8] as follows⁶:

$$\Delta_{Xmax} = 3(\Delta_M + \Delta_S) \quad (1)$$

Computer model of object is composed from many single points close to each other on its surface, as shown on Fig. 5. Every point is measured with uncertainty Δ_{Xmax} , so the maximal absolute volumetric uncertainty Δ_V is an spatial area marked on Fig. 5 with dashed lines and expressed as:

$$\Delta_V = S \cdot \Delta_{Xmax} \quad (2)$$

where S is surface area of the measured object [m^2]. Relative accuracy (δ_V) is then defined as:

$$\delta_V = \frac{S}{V} \cdot \Delta_{Xmax} \quad (3)$$

where V is volume of the measured object [m^3].

Since Robotic 3D Scanner is working with various manipulators and laser scanners, also final accuracy δ_V will vary for different constitutions. For body-part volumetric measurements, we use laser scanner MicroEpsilon ScanCONTROL2750-100 with accuracy $\Delta_S = \pm 0.027$ mm [64] and robotic manipulator Epson C3 with accuracy of end-point placement $\Delta_M = \pm 0.013$ mm [65]. According to (1), Robotic 3D Scanner's accuracy in this case is $\Delta_{Xmax} = \pm 0.12$ mm and according to (3), real volumetric measurement uncertainty (δ_{Vr}) of proposed device is:

$$\delta_{Vr} = \frac{S}{V} \cdot 1.2 \cdot 10^{-4} \quad (4)$$

VI. COMPARISON WITH STANDARD METHODS

Relative accuracies of all compared methods are summarized in Table I. Since relative accuracy of several methods is not a constant, it is not possible to clearly compare them

⁶This equation encapsulates also the uncertainty of Robotic 3D Scanner calibration procedure and it is a very pessimistic estimation – see [8].

TABLE I
METHODS COMPARISON: RELATIVE ACCURACIES OF STANDARD METHODS AND THE NEW METHOD.

Method	Relative Accuracy δ_V
Frustum Sign Model	8 %
Disc Model	6 %
Water Displacement Method	from 2 % (at 2700 cm^3) up to 8 % (at 25 cm^3)
Optoelectronic Volumeters	2 % (1000 – 3000 cm^3)
3D Ultrasonography	$(5.0 \cdot 10^{-3} \cdot S/V)$ %
Magnetic Resonance Imaging (MRI)	$(1.0 \cdot 10^{-3} \cdot S/V)$ %
Computed Tomography (CT)	$(2.0 \cdot 10^{-4} \cdot S/V)$ %
Robotic 3D Scanner	$(1.2 \cdot 10^{-4} \cdot S/V)$ %

directly. Because the value of accuracy is a function of measured object shape (more precisely function of surface-to-volume ratio), comparison will be made on two reference objects:

- **precise cuboid** – to be able to verify computed accuracy experimentally (see section VII),
- **human hand** – to be able to compare proposed method with standard ones in their standard working conditions.

Relative accuracy progressions of particular methods are visualized on Fig. 6 (for reference cuboid) and on Fig. 7 (for human hand). These progressions encapsulate the influence of surface-area-to-volume ratios (S/V) on relative accuracy of method.

It is clear from both figures, that accuracy of Robotic 3D Scanner reach the best value in every situation. The second most accurate method is computing the volume from CT captured model, but due to high doses of ionizing radiation, it is used very rarely. The third best method – Water Displacement Volumetry – does not have such serious limitations. From this reason it is the most used standard method, but its accuracy is approximately 4 times lower than accuracy of Robotic 3D Scanner Volumetry.

VII. EXPERIMENTAL RESULTS

Theoretical estimation of accuracy derived in section V-B was experimentally verified on set of reference objects with

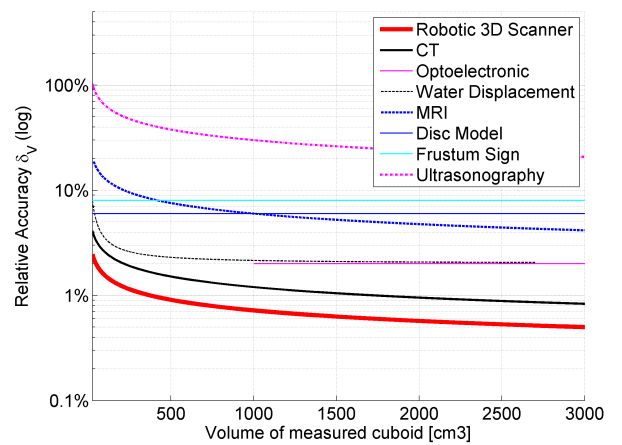


Fig. 6. Methods comparison: Relative measurement accuracy δ_V and its dependency on size of **cuboid** (its volume).

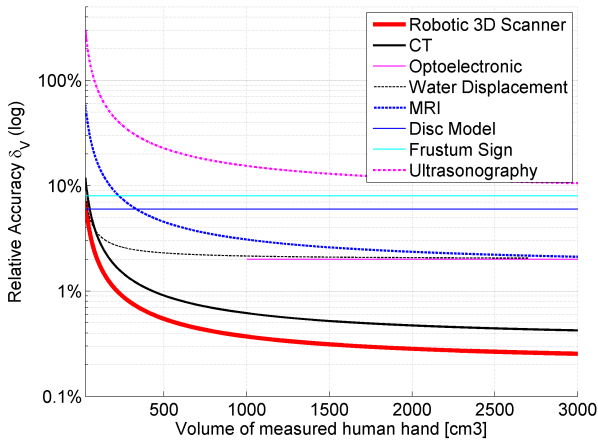


Fig. 7. Methods comparison: Relative measurement accuracy δ_V and its dependency on size of **human hand** (its volume).

known dimensions and volume. The first reference object was a precise cuboid from blackened steel manufactured by precision-engineering company and consequently verified in optical measuring chamber. Defining dimensions of cuboid are 29.996 ± 0.001 mm, 39.990 ± 0.001 mm and 49.993 ± 0.001 mm, with parallelisms of corresponding planes 0.005 ± 0.001 mm, 0.008 ± 0.001 mm and 0.007 ± 0.001 mm, and with maximal perpendicularity 0.007 ± 0.001 mm ($\vartheta = 22^\circ$ C, $\phi = 46\%$).

According to [66], true volume of the reference object V_{ref} is:

$$V_{ref} = 59.969 \pm 0.005 \text{ cm}^3 \quad (5)$$

Volume of this reference object was 10 times measured by Robotic 3D Scanner Volumetric Method. At each measurement, same scanning trajectory, but different orientation of reference object inside scanning area was used. The mean value and uncertainty type A [67] were determined from measured data:

$$V_{meas} = 60.43 \pm 0.30 \text{ cm}^3 \quad (6)$$

Assuming the equation (4), theoretical relative accuracy in case of measurement of object with this size is $\delta_{theory} = \pm 1.88\%$, so the measured value V_{meas} should be compatible with interval defined by true value V_{ref} and range δ_{theory} :

$$V_{theory} = 59.97 \pm 1.13 \text{ cm}^3 \quad (7)$$

This experiment proves validity of equation (4) for similar-sized objects since V_{meas} is compatible with V_{theory} .

To be able to verify wider range of volumes beyond the precise metal reference object, we used also the bigger reference cuboids. These objects were less-precise and made from wood (due to manufacturing expenses), but its dimensions were known together with uncertainty of dimension measurements. Results of these measurements were evaluated exactly the same way.

All results of verification are summarized in Table II and Fig. 8. All the relevant results are compatible, so the theoretically derived relative accuracy defined by equation (4) was verified and seems to be valid.

Figure 8 shows theoretical accuracy ("Declared accuracy") and true accuracy⁷ with errorbars presenting variance of measurements ("True accuracy"). Entire set of measured values stayed below the declared accuracy, what shows, that this accuracy estimation is very pessimistic, and real accuracy seems to be better ("Apparent real accuracy").

TABLE II
EXPERIMENTAL VERIFICATION OF METHOD ACCURACY.

Ref. Obj.	V_{ref} [cm ³]	δ_{Vr} [%]	V_{theory} [cm ³]	V_{meas} [cm ³]	Compatibility
#1	59.97	1.88	60.0 ± 1.1	60.4 ± 0.3	YES
#2	536.01	0.89	536.0 ± 4.8	535.1 ± 2.6	YES
#3	973.59	0.73	973.6 ± 7.1	974.8 ± 2.3	YES
#4	1734.71	0.63	1734.7 ± 11.0	1737.7 ± 3.0	YES
#5	2540.44	0.59	2540.4 ± 15.0	2544.4 ± 3.0	YES

VIII. CONCLUSION

Despite rapid development of 3D scanning, its boom impacts more or less only technically-oriented domains. But there are many opportunities also in other areas, like a medicine. This paper analyses needs of medicine in sense of 3D scanning and inferences requirements on medical 3D scanning. According this specification, medical 3D scanner has been developed and its contribution has been demonstrated on one of its applications – medical volumetry.

Proposed novel method for volumetric measurements reaches up to the best accuracy compared to all standard methods. According to pessimistic theoretical evaluations of performance, its relative accuracy varies from $\pm 1\%$ to $\pm 0.5\%$, depending on complexity of scanned limb surface, specifically on the surface-area-to-volume ratio. But during

⁷computed as relative difference between true (reference) value and measured value

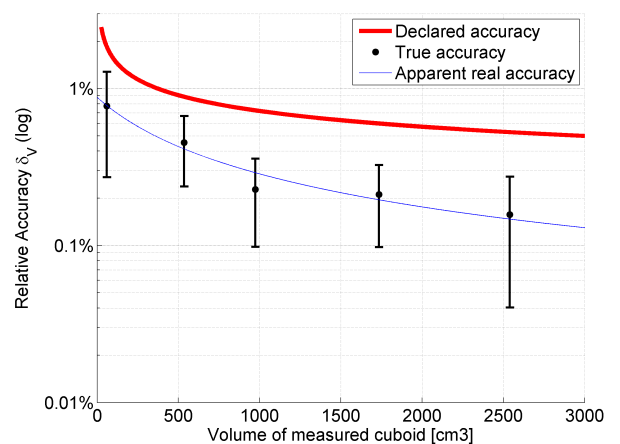


Fig. 8. Comparing verification measurements and theoretical method accuracy.

verifying experiments, relative error was even 4 times lower. The only area, where this method is not suitable is measurement of objects smaller than 1 cm^3 , where measurement error reaches up to $\pm 10 \%$.

In addition to high accuracy, proposed Robotic 3D Scanner is multi-purpose device having wide are of usage also outside of medical domain. It can be used in rescue robotics [68] or experimental biology [69]. In future work, it could be developed with more sensors with data fusion [70], what would allow not only monitoring the oedema, but also find the centre of inflammation due to augmented reality [71].

REFERENCES

- [1] "Google trends," <https://www.google.com/trends>. [Online]. Available: <https://www.google.com/trends>
- [2] "A roundup of how today's 3D printing technology is progressing." [Online]. Available: <http://3dprint.com/27954/3d-printing-roundup/>
- [3] "Digital underground," <http://www.metmuseum.org/about-the-museum/museum-departments/office-of-the-director/digital-media-department/digital-underground>. [Online]. Available: <http://www.metmuseum.org/about-the-museum/museum-departments/office-of-the-director/digital-media-department/digital-underground>
- [4] J. Park, "Digital restoration of seokguram grotto: The digital archiving and the exhibition of south korea's representative UNESCO world heritage," in *Proceedings of 2012 International Symposium on Ubiquitous Virtual Reality, ISUVR 2012*, 2012, pp. 26–29.
- [5] L. Zalud, L. Kopecny, and F. Burian, "Orpheus reconnaissance robots," in *Proceedings of the 2008 IEEE International Workshop on Safety, Security and Rescue Robotics, SSRR 2008*, Sendai, Japan, 2008, pp. 31–34.
- [6] L. Zalud, "ARGOS - system for heterogeneous mobile robot teleoperation," in *2006 IEEE/RSJ International Conference on Intelligent Robots and Systems, IROS 2006*, Beijing, China, 2006, pp. 211–216.
- [7] J. Hu, Y. Cao, T. Wu, D. Li, and H. Lu, "High-resolution three-dimensional visualization of the rat spinal cord microvasculature by synchrotron radiation micro-CT," *Medical Physics*, vol. 41, no. 10, 2014.
- [8] A. Chromy and L. Zalud, "Robotic 3D scanner as an alternative to standard modalities of medical imaging," *SpringerPlus*, vol. 3, no. 1, p. 13, 2014. [Online]. Available: <http://www.springerplus.com/content/3/1/13>
- [9] S. Klein, M. Avery, G. Adams, S. Pollard, and S. Simske, "From scan to print: 3D printing as a means for replication," *HP Laboratories Technical Report*, no. 30, 2014.
- [10] F. Haase, C. Siewert, D. B. von Rautenfeld, J. U. Fischbach, and H. Seifert, "Comparison of different methods to quantify the volume of horse limbs," *Berliner Und Mnchener Tierzliche Wochenschrift*, vol. 122, no. 3-4, pp. 126–131, Apr. 2009, PMID: 19350812.
- [11] S. H. Ridner, L. D. Montgomery, J. T. Hepworth, B. R. Stewart, and J. M. Armer, "Comparison of upper limb volume measurement techniques and arm symptoms between healthy volunteers and individuals with known lymphedema," *Lymphology*, vol. 40, no. 1, pp. 35–46, Mar. 2007, PMID: 17539463.
- [12] R. C. B. Ribeiro, S. M. P. F. Lima, A. C. G. Carreira, D. Masiero, and T. R. Chamlian, "Inter-tester reliability assessment of the volumetric measurement of the hand in subjects without any changes in their upper extremities," *Acta Fisiatrica*, vol. 17, no. 1, pp. 3–7, 2010. [Online]. Available: http://www.actafisiatrica.org.br/audiencia_pdf.asp?aid2=68&nomeArquivo=en_v17n1a02.pdf
- [13] D. M. Kaulsar Sukul, P. T. den Hoed, E. J. Johannes, R. van Dolder, and E. Benda, "Direct and indirect methods for the quantification of leg volume: comparison between water displacement volumetry, the disk model method and the frustum sign model method, using the correlation coefficient and the limits of agreement," *Journal of Biomedical Engineering*, vol. 15, no. 6, pp. 477–480, Nov. 1993, PMID: 8277752.
- [14] P. Konecny, "Nove trendy v neurorehabilitaci [abstract]," in *Dobsak P (ed) Proceedings of the IV. Dny Fyzioterapie: 11-12 October 2013*, 2013, pp. 7 – 7.
- [15] K. Lavelle and D. B. Stanton, "Measurement of edema in the hand clinic," May 2014.
- [16] J. M. Armer and S. H. Ridner, "Measurement techniques in assessment of lymphedema," *Lymph Link Article Reprint*, vol. 18, no. 3, pp. 1–4, Sep. 2006.
- [17] F. Brijker, Y. F. Heijdra, F. J. Van Den Elshout, F. H. Bosch, and H. T. Folgering, "Volumetric measurements of peripheral oedema in clinical conditions," *Clinical Physiology (Oxford, England)*, vol. 20, no. 1, pp. 56–61, Jan. 2000, PMID: 10651793.
- [18] T. Deltombe, J. Jamart, S. Recloux, C. Legrand, N. Vandebroek, S. Theys, and P. Hanson, "Reliability and limits of agreement of circumferential, water displacement, and optoelectronic volumetry in the measurement of upper limb lymphedema," *Lymphology*, vol. 40, no. 1, pp. 26–34, Mar. 2007, PMID: 17539462.
- [19] P. Karakas and M. G. Bozkir, "Anthropometric indices in relation to overweight and obesity among turkish medical students," *Archives of Medical Science*, vol. 8, no. 2, pp. 209–213, Apr. 2012, WOS:000304232700005.
- [20] R. Damstra, *Diagnostic and therapeutical aspects of lymphedema*. Drachten; Maastricht: Stichting Lymfologie Centrum Nederland (SLCN) ; University Library, Universiteit Maastricht [host], 2009.
- [21] A. R. Webb, *Introduction to biomedical imaging*. Hoboken, New Jersey: Wiley, 2003.
- [22] J. K. Udupa and G. T. Herman, *3D Imaging in Medicine, Second Edition*. CRC Press, Sep. 1999.
- [23] J. W. Ramsay, P. J. Barrance, T. S. Buchanan, and J. S. Higginson, "Paretic muscle atrophy and non-contractile tissue content in individual muscles of the post-stroke lower extremity," *Journal of Biomechanics*, vol. 44, no. 16, pp. 2741–2746, Nov. 2011. [Online]. Available: <http://linkinghub.elsevier.com/retrieve/pii/S0021929011005884>
- [24] M. d. A. Silva-Couto, C. L. Prado-Medeiros, A. B. Oliveira, C. C. Alcantara, A. T. Guimaraes, T. d. F. Salvini, R. Mattioli, and T. L. de Russo, "Muscle atrophy, voluntary activation disturbances, and low serum concentrations of IGF-1 and IGFBP-3 are associated with weakness in people with chronic stroke," *Physical Therapy*, vol. 94, no. 7, pp. 957–967, Jul. 2014, WOS:000338170100006.
- [25] W. Chong and P. Sidhu, *Measurement in Ultrasound: A practical handbook*. CRC Press, Apr. 2004.
- [26] P. Benington, "Masseter muscle volume measured using ultrasonography and its relationship with facial morphology," *The European Journal of Orthodontics*, vol. 21, no. 6, pp. 659–670, Dec. 1999. [Online]. Available: <http://ejo.oupjournals.org/cgi/doi/10.1093/ejo/21.6.659>
- [27] C. H. McCollough and F. E. Zink, "Performance evaluation of a multi-slice CT system," *Medical Physics*, vol. 26, no. 11, pp. 2223–2230, Nov. 1999, PMID: 10587202.
- [28] Statni urad pro jadernou bezpecnost, "Vyhlasaka o radiacni ochrane," 2002.
- [29] Z. Seidl and M. Vankov, *Magnetick rezonance hlavy, mozku a ptee*, avicenum ed. Grada, 2007. [Online]. Available: <http://www.martinus.cz/?uItem=32926>
- [30] "Coordinate measuring machine history - fifty years of CMM history leading up to a measuring revolution." [Online]. Available: <http://www.coord3-cmm.com/50-years-of-coordinate-measuring-machine/industry-developments-and-history/>
- [31] J. Shan and C. K. Toth, Eds., *Topographic laser ranging and scanning: principles and processing*. Boca Raton: CRC Press/Taylor & Francis Group, 2009.
- [32] K. B. Smith and Y. F. Zheng, "Accuracy analysis of point laser triangulation probes using simulation," *Journal of Manufacturing Science and Engineering*, vol. 120, no. 4, pp. 736–745, Nov. 1998. [Online]. Available: <http://dx.doi.org/10.1115/1.2830214>
- [33] R. G. Dorsch, G. Husler, and J. M. Herrmann, "Laser triangulation: fundamental uncertainty in distance measurement," *Applied Optics*, vol. 33, no. 7, p. 1306, Mar. 1994. [Online]. Available: <http://www.opticsinfobase.org/abstract.cfm?URI=ao-33-7-1306>
- [34] R. Heinkelmann and H. Schuh, "Very long baseline interferometry: accuracy limits and relativistic tests," in *Relativity in Fundamental Astronomy: Dynamics, Reference Frames, and Data Analysis*, ser. Proceedings of the International Astronomical Union, vol. 5, Apr. 2009, p. 286290. [Online]. Available: http://journals.cambridge.org/article_S1743921309990524

- [35] R. Morano, C. Ozturk, R. Conn, S. Dubin, S. Zietz, and J. Nissano, "Structured light using pseudorandom codes," *IEEE Transactions on Pattern Analysis and Machine Intelligence*, vol. 20, no. 3, pp. 322–327, Mar. 1998.
- [36] K. Liu, Y. Wang, D. L. Lau, Q. Hao, and L. G. Hassebrook, "Dual-frequency pattern scheme for high-speed 3-D shape measurement," *Optics Express*, vol. 18, no. 5, p. 5229, Mar. 2010. [Online]. Available: <<http://www.opticsinfobase.org/abstract.cfm?URI=oe-18-5-5229>>
- [37] S. Zhang and P. S. Huang, "High-resolution, real-time three-dimensional shape measurement," *Optical Engineering*, vol. 45, no. 12, pp. 123 601–123 601–8, 2006. [Online]. Available: <<http://dx.doi.org/10.1117/1.2402128>>
- [38] J. Baqersad, J. Carr, T. Lundstrom, C. Niezrecki, P. Avitabile, and M. Slattery, "Dynamic characteristics of a wind turbine blade using 3D digital image correlation," in *Proc. SPIE 8348, Health Monitoring of Structural and Biological Systems 2012*, vol. 8348, San Diego, California, 2012, pp. 83 482I–83 482I–9. [Online]. Available: <<http://dx.doi.org/10.1117/12.915377>>
- [39] G. F. Marshall, Ed., *Handbook of optical and laser scanning*, ser. Optical engineering. New York: Marcel Dekker, 2004, no. 90.
- [40] F. Walkowski, R. Johnston, and N. Price, "Texture mapping for the FastSCAN hand-held laser scanner," in *Image and Vision Computing New Zealand, 2008. IVCNZ 2008. 23rd International Conference*, Nov. 2008, pp. 1–6.
- [41] K. Strobl, E. Mair, T. Bodenmuller, S. Kielhofer, W. Sepp, M. Suppa, D. Burschka, and G. Hirzinger, "The self-referenced DLR 3D-modeler," in *IEEE/RSJ International Conference on Intelligent Robots and Systems, 2009. IROS 2009*, Oct. 2009, pp. 21–28.
- [42] A. L. Reyes, J. M. Cervantes, and N. C. Gutierrez, "Low cost 3D scanner by means of a 1D optical distance sensor," *Procedia Technology*, vol. 7, pp. 223–230, 2013. [Online]. Available: <<http://www.sciencedirect.com/science/article/pii/S2212017313000297>>
- [43] Zhang, A., Hu, S., Chen, Y., Liu, H., Yang, F., and Liu, J., "Fast continuous 360 degree color 3D laser scanner," in *INTERNATIONAL ARCHIVES OF PHOTOGRAMMETRY REMOTE SENSING AND SPATIAL INFORMATION SCIENCES*, vol. 1, 2008, pp. 409–414.
- [44] A. Chromy and L. Zalud, "Novel 3D modelling system capturing objects with Sub-Millimetre resolution," *Advances in Electrical and Electronic Engineering*, vol. 12, no. 5, pp. 476–487, Dec. 2014. [Online]. Available: <<http://advances.utc.sk/index.php/AEEE/article/view/1123>>
- [45] R. M. Murray, Z. Li, S. S. Sastry, and S. S. Sastry, *A Mathematical Introduction to Robotic Manipulation*. CRC Press, Mar. 1994.
- [46] S. Y. Nof, *Handbook of Industrial Robotics*. John Wiley & Sons, 1999.
- [47] F. Solc and L. Zalud, *Robotika*. Brno: Brno University of Technology, 2006.
- [48] L. G. Brown, "A survey of image registration techniques," *ACM Comput. Surv.*, vol. 24, no. 4, p. 325376, Dec. 1992. [Online]. Available: <<http://doi.acm.org/10.1145/146370.146374>>
- [49] P. Besl and N. D. McKay, "A method for registration of 3-D shapes," *IEEE Transactions on Pattern Analysis and Machine Intelligence*, vol. 14, no. 2, pp. 239–256, Feb. 1992.
- [50] S. Rusinkiewicz and M. Levoy, "Efficient variants of the ICP algorithm," in *Third International Conference on 3-D Digital Imaging and Modeling, 2001. Proceedings*, 2001, pp. 145–152.
- [51] Alshawa, M., "ICL: iterative closest line - a novel point cloud registration algorithm based on linear features," *Ekscentar*, no. 10, pp. 53–59, 2007.
- [52] J. Poppinga, N. Vaskevicius, A. Birk, and K. Pathak, "Fast plane detection and polygonalization in noisy 3D range images," in *IEEE/RSJ International Conference on Intelligent Robots and Systems, 2008. IROS 2008*, Sep. 2008, pp. 3378–3383.
- [53] F. Bellocchio, N. A. Borghese, S. Ferrari, and V. Piuri, *3D Surface Reconstruction*. New York, NY: Springer New York, 2013. [Online]. Available: <<http://link.springer.com/10.1007/978-1-4614-5632-2>>
- [54] K. Strobl, E. Mair, and G. Hirzinger, "Image-based pose estimation for 3-D modeling in rapid, hand-held motion," in *2011 IEEE International Conference on Robotics and Automation (ICRA)*, May 2011, pp. 2593–2600.
- [55] B. Mehta and R. Marinescu, "Comparison of image generation and processing techniques for 3D reconstruction of the human skull," in *Proceedings of the 23rd Annual International Conference of the IEEE Engineering in Medicine and Biology Society, 2001*, vol. 4, 2001, pp. 3687–3690 vol.4.
- [56] D. Chwa, J. Kang, and J. Choi, "Online trajectory planning of robot arms for interception of fast maneuvering object under torque and velocity constraints," *IEEE Transactions on Systems, Man and Cybernetics, Part A: Systems and Humans*, vol. 35, no. 6, pp. 831–843, Nov. 2005.
- [57] J. Levinson, J. Askeland, J. Becker, J. Dolson, D. Held, S. Kammel, J. Kolter, D. Langer, O. Pink, V. Pratt, M. Sokolsky, G. Stanek, D. Stavens, A. Teichman, M. Werling, and S. Thrun, "Towards fully autonomous driving: Systems and algorithms," in *2011 IEEE Intelligent Vehicles Symposium (IV)*, Jun. 2011, pp. 163–168.
- [58] G. Xiaoqing and W. Jidong, "Trajectory planning theory and method of industrial robot," in *2011 3rd International Conference on Computer Research and Development (ICCRD)*, vol. 2, Mar. 2011, pp. 340–343.
- [59] R. Danescu, "Obstacle detection using dynamic Particle-Based occupancy grids," in *2011 International Conference on Digital Image Computing Techniques and Applications (DICTA)*, Dec. 2011, pp. 585–590.
- [60] N. Fairfield and D. Wettergreen, "Evidence grid-based methods for 3D map matching," in *IEEE International Conference on Robotics and Automation, 2009. ICRA '09*, May 2009, pp. 1637–1642.
- [61] H. Yang and J. Chen, "Point cloud data enhancement based on layer connected region," in *2014 International Conference on Audio, Language and Image Processing (ICALIP)*, Jul. 2014, pp. 600–604.
- [62] A. Chromy, P. Kocmanova, and L. Zalud, "Creating Three-Dimensional computer models using robotic manipulator and laser scanners," in *12th IFAC Conference on Programmable Devices and Embedded Systems (2013)*, ser. Programmable devices and systems. Velke Karlovice: Elsevier B.V., Sep. 2013, pp. 268–273. [Online]. Available: <<http://www.ifac-papersonline.net/Detailed/62529.html>>
- [63] C. Zhang and T. Chen, "Efficient feature extraction for 2D/3D objects in mesh representation," in *2001 International Conference on Image Processing, 2001. Proceedings*, vol. 3, 2001, pp. 935–938 vol.3.
- [64] Micro-Epsilon, "Instruction manual scanCONTROL," 2008. [Online]. Available: <<http://www.micro-epsilon.cz/download/manuals/man--scanCONTROL-2700--en.pdf>>
- [65] Epson Robots, "Epson c3 compact 6-Axis RobotManual," 2011. [Online]. Available: <[http://robots.epson.com/admin/uploads/product_catalog/files/EPSON_C3_Robot_Manual\(R7\).pdf](http://robots.epson.com/admin/uploads/product_catalog/files/EPSON_C3_Robot_Manual(R7).pdf)>
- [66] T. Jamerson, "Uncertainty example using simple propagation of uncertainty rules," Aug. 2009.
- [67] R. Palencar, F. Vdolecek, and M. Halaj, "Nejistoty v mereni ii: nejistoty primych mereni," *Automa*, vol. 2001, no. 10, pp. 55–56, 2001.
- [68] L. Zalud, L. Kopecny, F. Burian, and T. Florian, "CASSANDRA - heterogeneous reconnaissance robotic system for dangerous environments," in *2011 IEEE/SICE International Symposium on System Integration, SII 2011*, 2011, pp. 1275–1280.
- [69] L. Nejdil, J. Kudr, K. Cihalova, D. Chudobova, M. Zurek, L. Zalud, L. Kopecny, F. Burian, B. Ruttkay-Nedecky, S. Krizkova, M. Konecna, D. Hynek, P. Kopel, J. Prasek, V. Adam, and R. Kizek, "Remote-controlled robotic platform ORPHEUS as a new tool for detection of bacteria in the environment," *Electrophoresis*, vol. 35, no. 16, pp. 2333–2345, 2014.
- [70] L. Zalud and P. Kocmanova, "Fusion of thermal imaging and CCD camera-based data for stereovision visual telepresence," in *2013 IEEE International Symposium on Safety, Security, and Rescue Robotics, SSR 2013*, 2013.
- [71] P. Kocmanova, L. Zalud, and A. Chromy, "3D proximity laser scanner calibration," in *2013 18th International Conference on Methods and Models in Automation and Robotics (MMAR)*, Aug. 2013, pp. 742–747.